# Undergraduate experiment with fractal diffraction gratings

**Juan A Monsoriu**[1,4]**, Walter D Furlan**[2]**, Amparo Pons**[2]**,
Juan C Barreiro**[2] **and Marcos H Giménez**[3]

[1] Centro de Tecnologías Físicas, Universitat Politècnica de València, E-46022 Valencia, Spain
[2] Departamento de Óptica, Universitat de València, E-46100 Burjassot, Valencia, Spain
[3] Instituto de Matemática Multidisciplinar, Universitat Politècnica de València, E-46022 Valencia, Spain

E-mail: jmonsori@fis.upv.es

**Abstract**
We present a simple diffraction experiment with fractal gratings based on the triadic Cantor set. Diffraction by fractals is proposed as a motivating strategy for students of optics in the potential applications of optical processing. Fraunhofer diffraction patterns are obtained using standard equipment present in most undergraduate physics laboratories and compared with those obtained with conventional periodic gratings. It is shown that fractal gratings produce self-similar diffraction patterns which can be evaluated analytically. Good agreement is obtained between experimental and numerical results.

(Some figures in this article are in colour only in the electronic version)

## 1. Introduction

When diffraction optics is introduced in first courses of physics, the structures considered are typically single slits, double slits and periodic grating (PGs). These are classic examples of objects used to teach diffraction phenomena but they are rarely used to show the potential application of diffraction in signal processing, for instance, important and relevant aspects of image processing (spatial filtering) [1]. In our opinion, non-conventional diffractive objects such as fractals could be used for this purpose.

Fractal geometry is exceptionally fruitful and has also been identified in many other scientific areas such as biology, medicine, electronics, geomorphology, and even stock markets. Mathematically, the concept of fractal is associated with a geometrical object which (i) is self-similar (i.e. the object is exactly or approximately similar to a part of itself) and (ii) has a fractional (or noninteger) dimension [2]. Fractals are obtained by performing a basic operation, called a *generator*, on a given geometrical object called an *initiator*. By sequentially repeating

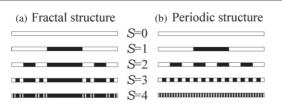[4] Author to whom any correspondence should be addressed.

**Figure 1.** (a) Triadic Cantor set at different stages of growth $S$ and (b) the equivalent periodic structure obtained by filling the fractal set with some segments.

this process on each one of the parts resulting from the operation, a multiple-level object, composed of sub-units of itself, is created that resembles the structure of the whole object [3].

In optics, fractal structures ranging from simple one-dimensional (1D) systems [4, 5] to complex 2D objects [6, 7] have been extensively studied. Specifically, diffraction gratings based on the fractal Cantor set sequences have been analysed [8, 9]. The fractal profile of these structures leads to Fraunhofer diffraction patterns with self-similar properties, i.e. the variation of the Fourier spectrum with spatial frequency at each higher stage is a modulated version of that associated with the previous step with an appropriate scaling of the frequency range. As a consequence of this fractal property, these structures exhibit a certain number of subsidiary diffraction peaks around the main peaks. This self-similar property has also been obtained with other diffractive optical elements, for example, with different kinds of fractal diffractive lenses [10, 11].

In this paper we present a simple experiment to verify the self-similar properties of Fraunhofer diffraction patterns produced by fractal gratings (FGs) with standard equipment present in most undergraduate physics laboratories. For comparison, the Fraunhofer patterns of regular PGs are also obtained. From a didactic point of view, the experiment developed is very motivating because it is also a way to introduce students to basic research activities.

## 2. Fractal gratings based on the triadic Cantor set

One of the simplest fractals is the triadic Cantor set, shown in figure 1(a), which can be obtained by means of an iterative construction. The first step ($S = 0$) is to define a segment of unit length. The next ($S = 1$) is to divide the segment in three equal parts of length 1/3 and remove the central one. The ternary set is created by repeating this process to infinity on the remaining segments.

The triadic Cantor set contains all points in the interval [0, 1] that are not deleted at any step in this infinite process. In general, at the stage $S$, there are $2^S$ segments of length $3^{-S}$ with $2^S - 1$ gaps in between. In figure 1(a), only the four first stages are shown for clarity. Note that the $S$th stage Cantor set can be interpreted as a quasiperiodic distribution of segments which can be obtained by removing some segments in a finite periodic distribution as shown in figure 1(b). This distribution at stage $S$ has $(3^S + 1)/2$ segments of length $3^{-S}$, separated by gaps of the same length, so the period of this finite structure is $\Lambda = 2 \times 3^{-S}$.

Based on the above scheme we propose FGs composed of slits distributed according to the triadic Cantor set, as shown in figure 2. In order to show the self-similarity properties of the diffracted field for different values of $S$ we have scaled the whole structure leaving in each stage the slits with the same width $a$. In this way the spacing between the diffraction orders will be preserved. Therefore, in our objects the grating length is given by $L = a \, 3^S$ and the
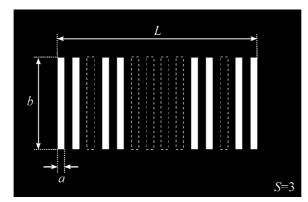
**Figure 2.** Fractal grating based on the triadic Cantor set (shown in figure 1) at the stage of growth $S = 3$. The dashed lines define the complimentary slits of the equivalent periodic grating.

period of the equivalent PG is $\Lambda = 2a$ (see figure 2). In mathematical terms, a Cantor grating of order $S$ can be represented by a binary function transmittance $t_F(x, y)$ given by

$$t_F(x, y) = \prod_{i=0}^{S} \text{rect}\left(\frac{\text{mod}\left[x - \frac{L}{2} + 3^i a, 2 \cdot 3^i a\right]}{2 \cdot 3^i a}\right) \text{rect}\left(\frac{x}{L}\right) \text{rect}\left(\frac{y}{b}\right), \qquad (1)$$

where $\text{rect}(x) = 1$ for $|x| < 1/2$ and 0 otherwise. In this equation $\text{mod}(x, y)$ gives the remainder on division of $x$ by $y$. The transmittance of the equivalent PG (represented in figure 2 by the dashed lines, slits plus the FG) is given by

$$t_P(x, y) = \text{rect}\left(\frac{\text{mod}\left[x - \frac{L}{2} + a, 2a\right]}{2a}\right) \text{rect}\left(\frac{x}{L}\right) \text{rect}\left(\frac{y}{b}\right). \qquad (2)$$

## 3. Theoretical Fraunhofer diffraction patterns

Let us consider a diffraction grating with transmittance $t(x,y)$, illuminated by a monochromatic plane wave (with wavelength $\lambda$). The Fraunhofer diffraction pattern is generated at the back focal plane of a lens placed against the grating. Within the scalar approximation, the focal irradiance distribution is given by the Fourier transform of the transmittance function [12]

$$I(x, y) = \left(\frac{A}{\lambda f}\right)^2 \left|\int_{-\infty}^{\infty} t(x_o, y_o) \exp\left(-i\frac{2\pi}{\lambda f}(x \cdot x_o + y \cdot y_o)\right) dx_o\, dy_o\right|^2, \qquad (3)$$

where $f$ is the focal length of the lens and $A$ is the amplitude of the incident plane wave. To compare the diffraction properties of an FG with its associated PG, we will obtain analytically the Fraunhofer diffraction irradiance distributions by replacing in the above equation the transmittance function $t(x, y)$ by equations (1) and (2), respectively.

For the first case, by using the dimensionless transversal coordinates $u = \frac{a}{\lambda f}x$ and $v = \frac{b}{\lambda f}y$, and using the convolution theorem for the Fourier transform, equation (3) can be rewritten as

$$I_F(u, v) = \frac{1}{4^S} \prod_{i=1}^{S} \frac{\sin^2(4\pi u 3^{S-i})}{\sin^2(2\pi u 3^{S-i})} \text{sinc}^2(u) \text{sinc}^2(v). \qquad (4)$$
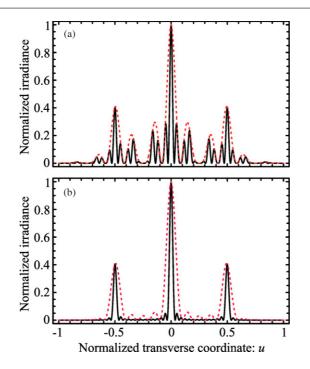
**Figure 3.** (a) Normalized Fraunhofer irradiance versus the transverse coordinate $u$ for an FG ($S = 2$; dashed curve and $S = 3$; solid curve) and (b) for its associated PG. In both cases $v = 0$.

For the associated PG, equation (3) leads to the well-known result [12]

$$I_P(u, v) = \frac{1}{M^2} \frac{\sin^2(M 2\pi u)}{\sin^2(2\pi u)} \operatorname{sinc}^2(u) \operatorname{sinc}^2(v). \qquad (5)$$

In equation (5) $M$ is the number of transparent slits and is given by $\left\lceil \frac{3^S}{2} \right\rceil$, where $\lceil x \rceil$, called the ceiling of $x$, denotes the smallest integer greater than or equal to $x$. Note that equations (4) and (5) have been normalized to $I(0,0) = 1$.

Profiles of the Fraunhofer irradiance produced by FGs with different stages of growth $S$ are shown in figure 3(a). The irradiance of the associated PGs is shown in the same figure for comparison. It can be seen that the main diffraction peaks in both cases coincide. However, the irradiance for the FG exhibits a characteristic fractal profile. It can also be noted that the irradiance for the FG at each higher stage is a modulated version of that associated with the previous stage. That is, the Fraunhofer diffraction pattern reproduces the self-similarity of the grating distribution.

## 4. Experimental results

The setup employed to experimentally obtain the Fraunhofer diffraction patterns is shown in figure 4. A He–Ne laser ($\lambda = 632.8$ nm) connected to the optical fibre is used as a point-source illuminator (A). A lens of focal distance $f = 200$ mm (B) collimates the beam. The diffraction gratings (C) were printed and then photographically reduced onto 35 mm slides. The sizes of the resulting slits are $a = 0.18$ mm and $b = 5.39$ mm. The Fraunhofer diffraction
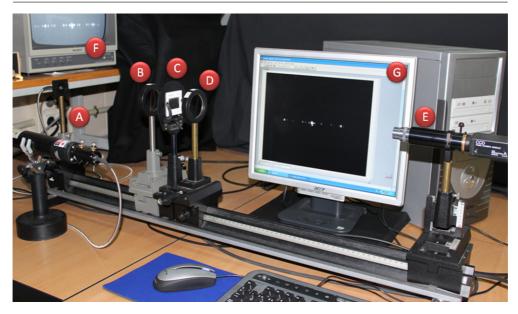
**Figure 4.** Experimental setup employed to obtain experimentally the Fraunhofer diffraction patterns.

patterns are obtained at the focal plane of the lens (D) ($f = 400$ mm). A microscope objective ($4\times$) forms an image of these diffraction patterns onto a CCD detector (E). The diffraction patterns can be visualized directly in the monitor (F) and by using image acquisition software, the patterns can be saved in the computer (G) as JPEG files (256-level grey scale and $764 \times 576$ pixels).

Figure 5 shows the experimental diffraction patterns obtained with FGs of orders $S = 2$ and $S = 3$ and the corresponding patterns obtained with the equivalent periodic structures. Although the patterns are recorded as images of $764 \times 576$ pixels, only the central regions of interest are shown in this figure. Note that the zero-order diffraction peaks are saturated in order to detect the high-order diffraction peaks. From figure 5, the self-similar behaviour of FGs is clear. In fact, any wide peak at stage $S = 2$ is transformed into three narrower peaks at stage $S = 3$ and nine peaks at stage $S = 4$ (not shown in figure 5). The image files are transformed with *Mathematica* in grey-level irradiance matrices, $I_{exp}(i, j)$, with $i = 1, 2, \ldots, 764$, $j = 1, 2, \ldots, 576$, and $0 \leqslant I_{exp} \leqslant 255$. Taking into account the symmetry properties of the diffraction patterns and using Mathematica's function Mean[*Position*[$I_{exp}$, Max[$I_{exp}$]]] it is easy to locate the central pixel, $(i_0, j_0)$, of the zero-order diffraction peak.

Focusing our attention only on the horizontal coordinate along the central axis $j = j_0$, the experimental data $I_{exp}(i, j_0)$ are fitted to the theoretical function $I_{th}(i, N, \gamma) = N \cdot I_F\left(\frac{i-i_0}{\gamma}, 0\right)$, where $N$ is a normalization factor and $\gamma$ is the scaling factor that transforms the horizontal coordinate $i$, defined in pixels, to frequencies $u = \frac{i-i_0}{\gamma}$. The parameters and their errors have been obtained according to the standard procedure of minimization of the $\chi^2$ merit function, defined as [13]

$$\chi^2(N, \gamma) = \sum_{i=1}^{764} \frac{(I_{exp}(i, j_0) - I_{th}(i, N, \gamma))^2}{\sigma_i^2}, \tag{6}$$
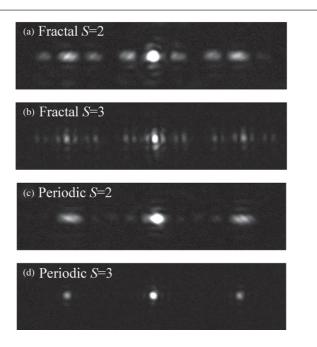
**Figure 5.** Experimental Fraunhofer diffraction patterns obtained with FGs of orders $S = 2$ and $S = 3$ and the corresponding periodic structures.
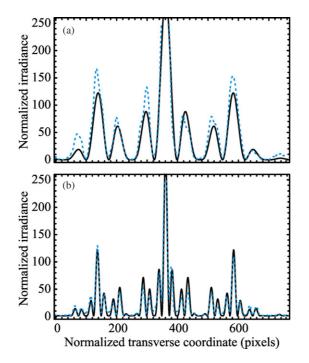


**Figure 6.** Experimental (dashed curve) and theoretical (solid curve) Fraunhofer diffraction patterns versus the transverse coordinate in pixels for FGs at (a) $S = 2$ and (b) $S = 3$.

**Table 1.** Experimental data fit.

|                                | Fractal $S = 2$        | Fractal $S = 3$        |
| ------------------------------ | ---------------------- | ---------------------- |
| Mean position $(i_0, j_0)$     | (361, 281) pixels      | (362, 274) pixels      |
| Normalization factor $N$       | $354.1 \pm 0.6$        | $299.1 \pm 0.8$        |
| Scale factor $\gamma$          | $(449.8 \pm 0.1)$ pixels | $(448.4 \pm 0.1)$ pixels |
| Regression coefficient         | 0.92                   | 0.91                   |

and by assigning an error of $\sigma = 3$ to the irradiance values corresponding to a mean noise registered. The points $i$ where the registered irradiance is saturated have not been considered in the above sum.

The dashed curves in figure 6 represent the experimental data obtained for the FGs at stages $S = 2$ and $S = 3$. The fitted functions are shown in the same figure with solid curves for comparison. The values of the fitted parameters are given in table 1. Good agreement is obtained between the theoretical and experimental data, the regression coefficient being higher than 0.9 in both fractal cases. Similar regression coefficients are obtained with the equivalent periodic structures (not shown in figure 6).

## 5. Conclusions

We have presented a simple optical method to analyse the Fraunhofer diffraction properties of one-dimensional gratings based on the Cantor set. With this method we have shown that optical processing can be performed using standard equipment available in most undergraduate physics laboratories. In fact, the self-similarity of the diffraction patterns can be easily observed and recorded with this setup and measurements of the mathematical properties of the Cantor are also possible from experimental results. It is worth mentioning that with this method other one-dimensional or two-dimensional fractals, such as polyadic Cantor sets, or other quasiperiodic structures, such as the Fibonacci gratings, can be studied. In our opinion, this result could motivate students to study further in the field of optical processing.

## Acknowledgments

## References

[1] Hetcht E 2002 *Optics* (San Francisco: Addison-Wesley)
[2] Mandelbrot B B 1982 *The Fractal Geometry of Nature* (San Francisco: Freeman)
[3] Ficker T and Benesovký P 2002 Deterministic fractals *Eur. J. Phys.* **23** 403
[4] Sakurada Y, Uozumi J and Asakura T 1992 Fresnel diffraction by 1-D regular fractals *Pure Appl. Opt.* **1** 29
[5] Trabocci O, Granieri S and Furlan W D 2001 Optical propagation of fractal fields. Experimental analysis in a single display *J. Mod. Opt.* **48** 1247
[6] Uozumi J, Peiponen K E, Savolainen M and Silvennoinen R 1994 Demonstration of diffraction by fractals *Am. J. Phys.* **62** 283

[7]   Jaggard A D and Jaggard D L 1998 Cantor ring diffractals *Opt. Commun.* **158** 141
[8]   Lehman M 2001 Fractal diffraction gratings built through rectangular domains *Opt. Commun.* **195** 11
[9]   Zunino L and Garavaglia M 2003 Fraunhofer diffraction by cantor fractals with variable lacunarity *J. Mod. Opt.* **50** 717
[10]  Saavedra G, Furlan W D and Monsoriu J A 2003 Fractal zone plates *Opt. Lett.* **28** 971
[11]  Monsoriu J A, Furlan W D, Saavedra G and Giménez F 2007 Devil's lenses *Opt. Express* **15** 13858
[12]  Goodman J W 1996 *Introduction to Fourier optics* (New York: McGraw-Hill)
[13]  Bevington P and Robinson D K 1993 *Data Reduction and Error Analysis for the Physical Sciences* (New York: McGraw-Hill)